JOURNAL OF THERMOPHYSICS AND HEAT TRANSFER
Vol. 18, No. 3, July–September 2004

Simultaneous Determination of Thermophysical Properties Using a Thermistor, Part 1: Numerical Model

Cherif Ould Lahoucine*
Georgia Institute of Technology, Atlanta, Georgia 30332-0405
and
Hiroto Sakashita† and Toshiaki Kumada‡
Hokkaido University, Sapporo 060-8628, Japan

A new thermistor-based technique for the measurement of thermophysical properties of liquids and porous materials is proposed. To simulate the real situation, a two-dimensional numerical thermal model of the thermistor, surrounded by a sample of cylindrical shape, is presented. The simultaneous estimation of thermal conductivity and diffusivity by the use of an inverse analysis is detailed. If the measured volume-averaged temperature rise of the thermistor is available, then thermal diffusivity of the sample is evaluated first from the plot of these measured temperatures vs the logarithm of the Fourier number. Once thermal diffusivity is evaluated, thermal conductivity is obtained through the minimization of standard deviation between calculated and experimental temperatures of the thermistor in the least-square sense. The time range used to determine the thermophysical properties is selected within the transient-state part of time-dependent temperature rise of thermistor, expressed in dimensionless form, and is situated between Fourier number $Fo = 1$ and $Fo = 10$. In addition, and to get accurate results, an analysis is performed to show the set of parameters to be adjusted before actual measurements. The parameters are the dimensions of the sample, time step, and the mesh sizes used in the numerical analysis.

Nomenclature

A = dimensionless coefficient in Eq. (12)
a = coefficient in Eq. (13), K
a' = coefficient in Eq. (14), K
B = dimensionless coefficient in Eq. (12)
b = coefficient in Eq. (13), K
b' = coefficient in Eq. (14), K
Fo = dimensionless time Fourier number
I = current supplied to the chip, A
L = length in axial direction, m
L_{ch} = length of the chip, m
L_w = immersion depth of thermistor, m
n = number of time steps
q = heat generated in the chip, W
q_v = heat generation rate per unit time and volume inside the chip, W/m^2
R = dimensionless radial coordinate
R_c = thermal conductivity ratio
R_d = thermal diffusivity ratio
R_s = dimensionless radius of the sample
R_w = dimensionless radius of the lead wire
r = radial coordinate, m
r_{ch} = radius of the chip, m
r_s = radius of the sample, m
T = temperature, K
t = time, s
V = voltage supplied to the chip, V
Z = dimensionless axial coordinate
Z_s = dimensionless length of the sample
Z_w = dimensionless immersion depth of thermistor
z = axial coordinate, m
α = thermal diffusivity, m^2/s
ΔFo = dimensionless time step
ΔR = dimensionless increment in radial direction
Δr = increment in radial direction, m
ΔZ = dimensionless increment in axial direction
Δz = increment in axial direction, m
δ = thickness of wire insulating material, m
θ = dimensionless temperature
λ = thermal conductivity, W/m · K
μ = deviation
σ = standard deviation, %

Subscripts

cal = calculated
ch = chip
est = estimated
exp = experimental
gl = glass protection of the chip
i = index of time domain
ini = initial state
inp = input
int = interface between two adjacent materials
n = number of time steps
new = new temperature
old = old temperature
s = sample
si = insulating material of the wire
ss = steady state
v = volume averaged
w = lead wire

Received 12 November 2003; revision received 11 February 2004; accepted for publication 13 February 2004. Copyright © 2004 by the American Institute of Aeronautics and Astronautics, Inc. All rights reserved. Copies of this paper may be made for personal or internal use, on condition that the copier pay the $10.00 per-copy fee to the Copyright Clearance Center, Inc., 222 Rosewood Drive, Danvers, MA 01923; include the code 0887-8722/04 $10.00 in correspondence with the CCC.

*Fulbright Visiting Scholar, George W. Woodruff School of Mechanical Engineering; cherif.ouldlahoucine@me.gatech.edu or koukra@hotmail.com. Member AIAA.
†Associate Professor, Department of Quantum Energy Engineering, Kita 13 Nishi 8, Kita-Ku.
‡Professor, Department of Quantum Energy Engineering, Kita 13 Nishi 8, Kita-Ku.

Introduction

THERMOPHYSICAL properties of materials are very important for the comprehension of thermal phenomena and the advancement of many scientific fields. Yet, among the materials available in nature, thermal conductivities of low-viscosity fluids,

liquid metals, powders, and porous materials are by far the most difficult to measure. However, the accurate measurement of thermophysical properties of some powders and porous materials is needed, such as these for the porous mineral aggregates in planetary science,[1] the alumina Al_2O_3 in space power systems,[2] the zeolites in hydrogen storage,[3] or the bentonite in nuclear engineering,[4] to name few. For the estimation of thermal properties, researchers used different techniques that varied depending on the nature of the sample, the temperature range, and the pressure during measurements.[5–7]

These techniques can be classified into two main categories: the steady-state and transient-state techniques. The nonsteady-state techniques are faster and generally more efficient and simpler to apply.[1] Presently, for powders, the thermal conductivity probe is considered the method of choice for field work; however, the transient hot wire is considered the preferred method in the laboratory.[1] Using it, many researchers have succeeded in determining the thermal conductivity of liquids,[8] gases, powders,[3,9] and even liquid metals[10,11] with acceptable accuracy. Each of these methods is based on the assumption of one-dimensional radial diffusion of heat from a line heat source, and the derivation of the solution is given by Carslaw and Jeager.[12] Detailed discussions about the errors in the thermal conductivity probe and transient hot-wire techniques can be found in the published papers of Blackwell,[13] Xin-Gang,[14] Jones,[15] and Griesinger et al.[16] A perfect line heat source is infinitely long and infinitely thin. The thermal conductivity probe deviates significantly from this ideal. A transient hot wire is much closer to being a "perfect" line heat source than is the probe, with length-to-diameter ratios > 500 being easy to achieve. The measurement time is also much shorter, thus, a smaller sample can be used. The typical volume used in the transient hot-wire method was about 13 ml (Refs. 3 and 9). This volume can be reduced further by the adoption of a short hot-wire technique assisted by numerical analysis, as was the case for the simultaneous measurement of thermal conductivity and diffusivity of liquids proposed by Fujii et al.[17] However, because of serious limitations in mechanical stability, the short hot-wire technique cannot be used for compacted powders. Instead, the thermal conductivity probe was used in most of the thermal conductivity measurements of particulate materials by Jones,[15] Woodside and Messmer,[18] Horai et al.,[19] and Seiferlin et al.[20] The accuracy has been reported at $\pm 10\%$ for conductivity greater than 0.1 $W/m \cdot K$, whereas for values listed hereafter, the accuracy is expected to be even lower than $\pm 10\%$ because, as Nicolas et al.[21] cautioned, low thermal conductivity standards do not exist, which, in turn, leads to an imperfect calibration of the probe. Horai et al.[19] used the composite circular cylinder apparatus to measure the thermal conductivity of lunar samples. They found standard deviations in the reported thermal conductivity values of about 20–40%. Moreover, for powders, cylinder or plate methods bring forth high-temperature differences between the hot and the cold wall (20–40 K), to achieve sufficient accuracy.[22] Thus, the thermal conductivity cannot be assigned to one certain temperature in these two methods, and, for a moist porous sample, this important temperature gradient will yield the migration of moisture from the hot region to the cold region within the sample. Hence, values obtained will not correspond to the conductivity of the sample's original moisture fraction.

In addition, the review by Presley and Christensen[1] reveals that, in the previously published data (including those under very low atmospheric pressure), the standard deviations are sometimes very high, accuracy better than $\pm 10\%$ is very difficult to achieve, and that, in some data, anomalous behavior and even a contrast such as that between the data of Wechsler and Glaser[23] and that of Fountain and West[24] can be found. This suggests that, for the measurement of thermal conductivity of particulate materials and soft powders, further studies would certainly be useful, and further investigation is needed to check the accuracy of the previously published data and to assess the relative advantage of one method over the other available transient techniques for laboratory measurement.

Because of its simple experimental setup, short time of measurement, high sensitivity, mechanical stability when used in highly compacted powder, and small test sample, the thermistor technique is suitable for laboratory measurements. Chato[25] was the first to use a thermistor for the measurement of thermal conductivity. The application was in the medical field, specifically, measuring the thermal conductivity of perfused biological tissue. Balasubramaniam and Bowman[26] proposed a much improved model to simultaneously determine the thermal conductivity and diffusivity of biomaterials. They assumed that the thermistor bead was a distributed spherical thermal mass composed of homogeneous material and kept its average temperature constant. However, the existence of two lead wires in the real thermistor and the effect of the conduction of heat along them, which becomes very important for low thermal conductivity materials, were ignored. Therefore, the estimated thermal conductivity was not very accurate.

To remedy the drawbacks in the traditional approach, the present work uses a numerical method to estimate thermal conductivity and thermal diffusivity simultaneously. The numerical temperature history is calculated after the two-dimensional cylindrical coordinates differential equation is transformed into a discrete form by the use of finite difference scheme. This is the first part of the process. The second part is an optimization carried out via a search for the minimum of the standard deviation between the numerical and the experimental temperatures histories in the least-square sense. This optimal solution will yield the best estimation of thermophysical properties of the unknown material. This method, called inverse estimation, has been used before to estimate thermal conductivity.[27,28]

The objective of this work is twofold: First, a new thermistor technique that was successfully applied by the authors for the estimation of thermal conductivity of bentonite powder[4] as a good alternative to the measurement of the thermophysical properties of powders, porous materials, and liquids in the laboratory is presented. Second, an analysis is performed to show the set of parameters to be adjusted before any measurement are taken to yield accurate results. The parameters are the dimensions of the sample, boundary conditions, time steps and the mesh sizes used in the numerical analysis. This paper and its companion[29] pave the way for a more effective utilization of this new technique of measurement.

Numerical Analysis

Figure 1 shows the real thermistor that will be used in the case of real measurements, as well as its simulated model. The type is PSB-S7 (Shibaura Electric Company, Inc.). It is used both as heater and resistance to measure its temperature variation. The shape of the thermistor chip is rectangular parallelepiped and the estimated dimensions are given by the maker as approximately 0.3 mm × 0.25 mm × 0.15 mm. The lead wires are dumet alloy with a diameter of 0.1 mm. For the measurement of electrically conducting or highly corrosive fluids, such as liquid metals, the lead wires are covered by an insulating material of thickness δ. The diameter and length of the glass covering the chip are about 0.6 and 1.0 mm, respectively.

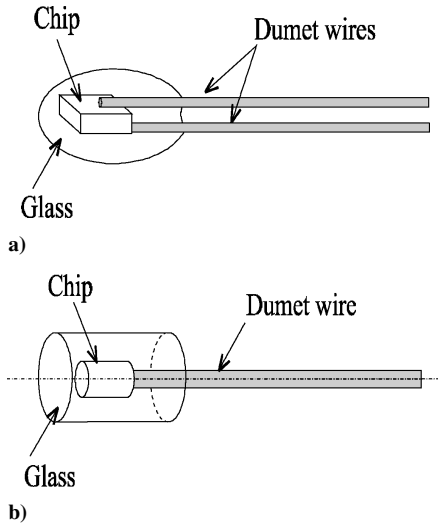

Fig. 1 Thermistor probes: a) real and b) simulated model.

In the simulated model, both the thermistor chip and its surrounding glass protection have a cylindrical shape. The differential equation for the thermistor bead inserted into a cylindrical container filled with a medium of unknown thermal conductivity, with corresponding initial and boundary conditions for a two-dimensional domain of calculation given in cylindrical coordinates, is given under the following assumptions:

1) The two-dimensional model cannot simulate the presence of the two wires, and only a single wire is considered. However, the conductance in the axial and the radial directions of the simulated single wire are considered equal to their corresponding values for the two real wires. The simulated single wire has twice the diameter and one-half of the thermal conductivity of the real wires.

2) The temperature field is two-dimensional and axisymmetric.

3) The thermophysical properties of all materials used in the calculations are temperature independent, homogeneous, and isotropic.

4) The heat generation rate per unit of time and volume is constant and uniformly distributed within the chip.

5) Initially, the thermistor probe and the sample were at uniform temperature T_{ini}.

6) The temperature at the boundaries is kept constant and equal to the initial temperature T_{ini}.

The dimensionless basic differential equations in cylindrical coordinates, and the corresponding boundary and initial conditions, are given in the following differential equations:

For the chip

$$\frac{\partial\theta_{\text{ch}}}{\partial Fo}=\frac{1}{R_{d_{\text{ch}}}}\cdot\left[\frac{\partial^2\theta_{\text{ch}}}{\partial R^2}+\frac{1}{R}\frac{\partial\theta_{\text{ch}}}{\partial R}+\frac{\partial^2\theta_{\text{ch}}}{\partial Z^2}\right]+\frac{R_{c_{\text{ch}}}}{R_{d_{\text{ch}}}} \tag{1}$$

For the glass

$$\frac{\partial\theta_{\text{gl}}}{\partial Fo}=\frac{1}{R_{d_{\text{gl}}}}\cdot\left[\frac{\partial^2\theta_{\text{gl}}}{\partial R^2}+\frac{1}{R}\frac{\partial\theta_{\text{gl}}}{\partial R}+\frac{\partial^2\theta_{\text{gl}}}{\partial Z^2}\right] \tag{2}$$

For the lead wire

$$\frac{\partial\theta_{w}}{\partial Fo}=\frac{1}{R_{d_{w}}}\cdot\left[\frac{\partial^2\theta_{w}}{\partial R^2}+\frac{1}{R}\frac{\partial\theta_{w}}{\partial R}+\frac{\partial^2\theta_{w}}{\partial Z^2}\right] \tag{3}$$

For the insulating layer

$$\frac{\partial\theta_{\text{si}}}{\partial Fo}=\frac{1}{R_{d_{\text{si}}}}\cdot\left[\frac{\partial^2\theta_{\text{si}}}{\partial R^2}+\frac{1}{R}\frac{\partial\theta_{\text{si}}}{\partial R}+\frac{\partial^2\theta_{\text{si}}}{\partial Z^2}\right] \tag{4}$$

For the sample

$$\frac{\partial\theta_{\text{s}}}{\partial Fo}=\left[\frac{\partial^2\theta_{s}}{\partial R^2}+\frac{1}{R}\frac{\partial\theta_{s}}{\partial R}+\frac{\partial^2\theta_{s}}{\partial Z^2}\right] \tag{5}$$

Boundary and initial conditions are

$$\theta(R,0,Fo)=\theta(R\geq R_w,Z_s,Fo)=\theta(R_s,Z,Fo)=0 \tag{6}$$

$$\frac{\partial\theta(0,Z,Fo)}{\partial R}=0,\qquad\frac{\partial^2\theta(R\leq R_w,Z_s,Fo)}{\partial Z^2}=0 \tag{7}$$

$$\theta(R,Z,0)=0 \tag{8}$$

where θ, R, and Z are the dimensionless temperature, radial, and axial coordinates, respectively. Fo is the dimensionless time or Fourier number. These are defined as

$$\theta=\frac{T-T_{\text{ini}}}{q_v r_{\text{ch}}^2/\lambda_s},\qquad R=\frac{r}{r_{\text{ch}}},\qquad Z=\frac{z}{r_{\text{ch}}}$$

$$Fo=\frac{\alpha_s t}{r_{\text{ch}}^2},\qquad R_s=\frac{r_s}{r_{\text{ch}}},\qquad R_w=\frac{r_w}{r_{\text{ch}}},\qquad Z_s=\frac{L_s}{r_{\text{ch}}} \tag{9}$$

The parameters $R_{d_{\text{ch}}}$, $R_{c_{\text{ch}}}$, etc., are the thermal diffusivity and conductivity ratios for each layer identified by the subscripts. These are defined as

$$R_{d_{\text{ch}}}=\alpha_s/\alpha_{\text{ch}},\qquad R_{d_{\text{gl}}}=\alpha_s/\alpha_{\text{gl}},\qquad R_{d_{\text{w}}}=\alpha_s/\alpha_w$$

$$R_{d_{\text{si}}}=\alpha_s/\alpha_{\text{si}},\qquad R_{c_{\text{ch}}}=\lambda_s/\lambda_{\text{ch}} \tag{10}$$

The partial differential equations (1–5) with the boundary and initial conditions (6–8) are solved numerically by the use of a finite differences scheme. After discretization, we obtain a set of algebraic equations that will be presented under the implicit second-order accurate in space and time Crank–Nicholson formulation. The solution can easily be performed by the use of the tridiagonal matrix algorithm (see Ref. 30) to give the simulated temperature time history for each node of the calculation domain. The calculations stopped when, for the same node, the absolute value of the difference between the newly estimated dimensionless temperature and the old one given by $|\theta_{\text{new}}-\theta_{\text{old}}|\leq 10^{-6}$ were satisfied. This should be done continuously until the whole dimensionless temperature–time history is calculated. When such a requirement is reached for all of the nodes, the algebraic mean dimensionless temperature of the chip is then calculated. This can be expressed as the sum of the dimensionless temperatures of all of the nodes within the thermistor chip, divided by the total number of those nodes. A nonuniform grid system is adopted, with a refinement within the thermistor chip and the glass covering (Fig. 2). The dimensionless mesh in the radial and axial directions are defined by $\Delta R=\Delta r/r_{\text{ch}}$ and $\Delta Z=\Delta z/r_{\text{ch}}$, respectively. The dimensionless time step is defined by $\Delta Fo=\alpha_m\Delta t/r_{\text{ch}}^2$.

To handle the abrupt change of conductivity that occurs at the interfaces between the two different materials comprising the thermistor probe, an interface thermal conductivity is prescribed. It represents the harmonic mean of the two thermal conductivities as proposed by Patankar.[30] As an example, at the interface between the glass and the chip placed midway between two adjacent nodes, the grid size is uniform; therefore, the thermal conductivity is given as

$$\lambda_{\text{int}}=\frac{2\lambda_{\text{gl}}\lambda_{\text{ch}}}{\lambda_{\text{gl}}+\lambda_{\text{ch}}} \tag{11}$$

To determine the whole dimensionless temperature history of the calculation domain, all of the thermophysical properties, as well as the dimensions of each component, should be known a priori and used as input values. The dimensions and thermophysical properties of the simulated thermistor presented in Fig. 1b are listed in Table 1.

Table 1 Thermophysical properties and estimated dimensions of thermistor probe

Material	Radius, mm	Length, mm	λ, W/m · K	$\alpha\times10^6$, m^2/s
Dumet wire	0.05	26	172	42.219
Thermistor chip	0.14	0.2	20	10.256
Insulating	Thickness	0.02	0.1	0.113
Glass protection	0.26	1.0	0.85	0.554

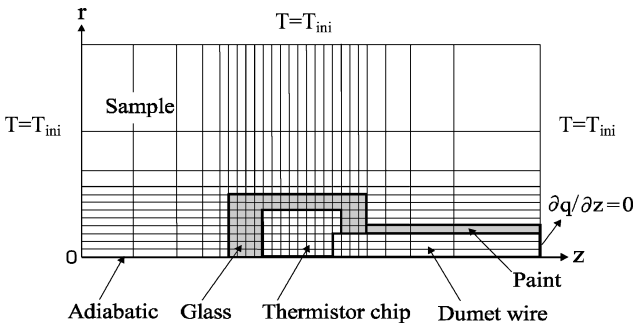

Fig. 2 Calculation domain with the selected grid and boundary conditions.

These dimensions and the thickness of the insulating material for the lead wires are determined by calibration, which is given in a separate paper.[29] The thermophysical properties are given by the thermistor's manufacturer.

Boundary Condition Effects

Numerical analysis yields the dimensionless volume-averaged chip temperature θ_v as a function of the dimensionless Fourier number. If heat is generated at a constant rate inside the chip of a thermistor bead initially at thermal equilibrium with its surrounding sample, the obtained temperature rise of the thermistor depends not only on the value of the heat generation rate, but also on the nature of the surrounding sample, the assumed perfect thermal contact between the thermistor and the sample, and the boundary conditions. A discussion of the effects of boundary conditions in both the radial and axial directions is important. Actually, those effects depend on the nature of the sample surrounding the thermistor because, for the same heat generation rate and volume of the sample, the lower the thermal conductivity of a sample is, the more the temperature rise of the thermistor becomes affected by the boundary conditions. An analysis is needed to clarify this point. It will yield the optimal size of the cylindrical container, which, in the case of a real measurement of the thermistor temperature rise, gives data free from boundary condition errors. Figure 3 shows the typical cell arrangement used for the present sensitivity analysis simulation. Mercury (high thermal conductivity) and glycerol (low thermal conductivity) are selected as the materials to be checked. In the following simulations, the heat generation rate is selected as equal to 8.2 mW, which can be typical of actual operation. In the present simulation, thermophysical properties for glycerol and mercury were taken from *JSME Data Book*[31] and Lide and Kehiaian,[32] respectively. The dimensionless length of the sample Z_s is selected as twice the dimensionless immersion depth of the thermistor Z_w, which is defined as $Z_w = L_w/r_{\mathrm{ch}}$, that is, $L_s = 2 \cdot L_w$, which means that the thermistor is inserted half way into the total height of the sample.

In the radial direction, the effect of the boundary condition at $R_s = r_s/r_{\mathrm{ch}}$ shows that, for $R_s \geq 5$, the dimensionless temperature of thermistor immersed in mercury or glycerol becomes independent of the boundary condition selected as shown in Figs. 4 and 5, respectively. These results were obtained by the use of a value for dimensionless immersion depth of the thermistor $Z_w = 50$. Note that, in a transient state, where the dimensionless volume-averaged temperature of the chip θ_v varies with the dimensionless time *Fo*, the location of the radial boundary condition has no effect on the dimensionless temperature–time history, and the curves corresponding to different values of the dimensionless radius R_s are similar. This provides confirmation that a measurement of thermal conductivity by the use of a transient state is the best choice because it avoids boundary errors but also saves time of calculation. In the axial direction, the influence of the boundary condition is more pronounced due to the presence of the lead wire. Figure 6 shows that, for mercury, $Z_w = 11$ is enough to achieve accurate measurement provided that the Fourier number is less than 30. However, Fig. 7 indicates that, for glycerol, Z_w needs to be increased to 44 to avoid boundary conditions errors. For both results, the dimensionless radius of the sample R_s was selected as $R_s = 5$. Globally, Figs. 4–7 indicate that the present thermistor technique requires a small sample of liquid or powder for the experiment.

The lead wire effects for mercury and glycerol are presented in Figs. 8 and 9, respectively. Figures 8 and 9 show that, if the diameter of the lead wire increases, as does the amount of the heat

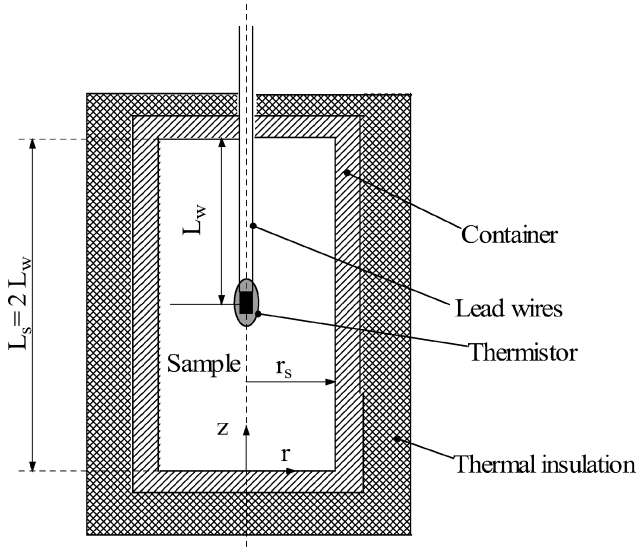

Fig. 3 Typical cell arrangement used for the sensitivity analysis.

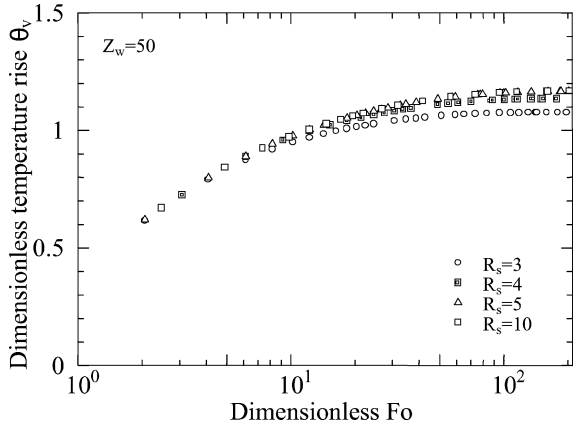

Fig. 4 Radial boundary condition effect for mercury.

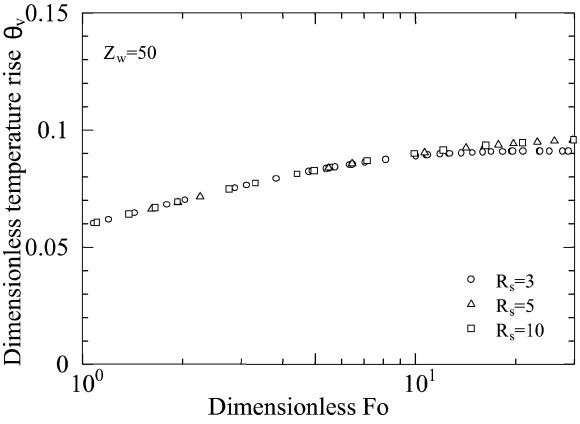

Fig. 5 Radial boundary condition effect for glycerol.

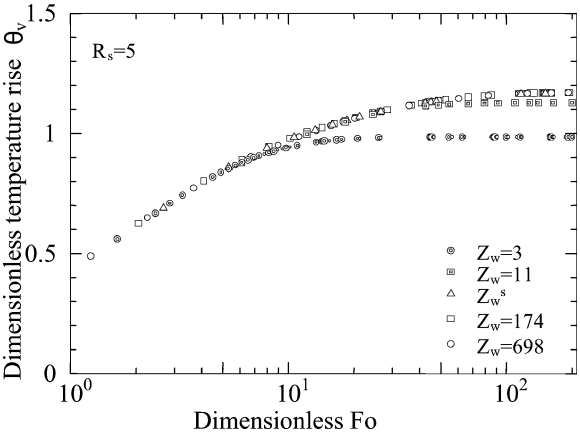

Fig. 6 Axial boundary condition effect for mercury.

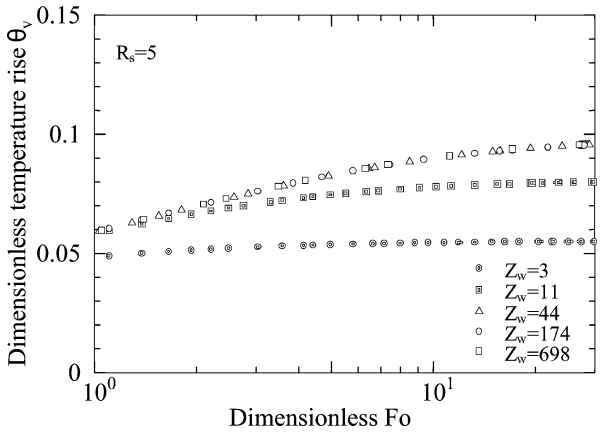

Fig. 7 Axial boundary condition effect for glycerol.

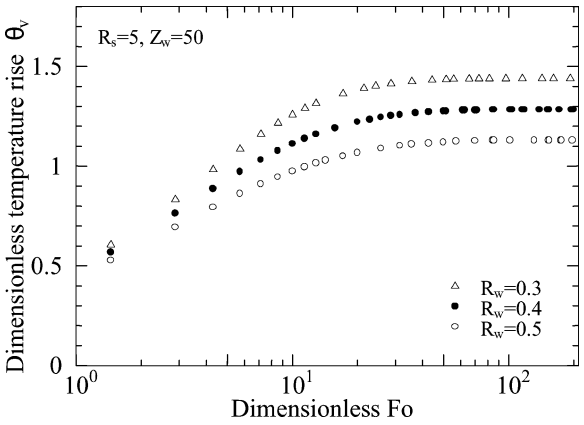

Fig. 8 Lead wire effect for mercury.

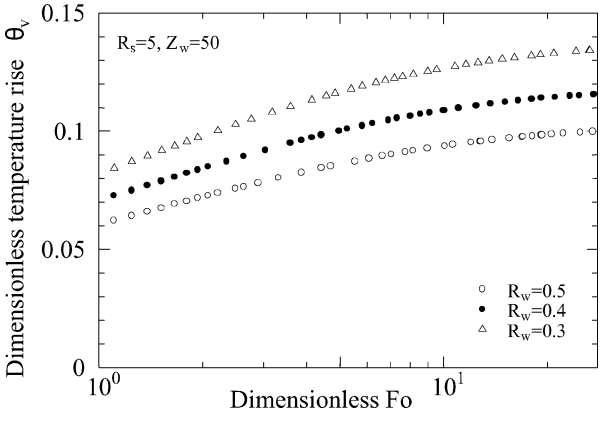

Fig. 9 Lead wire effect for glycerol.

conducted through the wire, the temperature rise of the chip decreases. This effect is more pronounced for glycerol, as can be noted, particularly in the transient state. In the conventional thermistor technique, thermal conductivity is determined by the use of an analytical formula, in which thermal conductivity is inversely proportional to the thermistor's temperature rise, which leads to an estimated value higher than the actual one. This error, called conduction lead wire error, is more pronounced when moderate to low thermal conductivity materials such as glycerol are measured. The present proposed method takes this effect into account, whereas the conventional method cannot evaluate it. These results are obtained using $Z_w = 50$ and $R_s = 5$, respectively. The dimensionless radius used for comparison is $R_w = r_w / r_{ch}$.

The numerical results presented in Figs. 4–9 depend on the dimensionless time steps ΔFo and mesh sizes in the radial and axial directions (ΔR and ΔZ) used in the numerical procedure. Various combinations were tested to check the accuracy of the present numerical results. Each combination provides a different dimensionless volume-averaged temperature rise of the thermistor chip. The standard deviations σ (%) of the difference between each solution and the optimal one are presented in Tables 2 and 3 for mercury and glycerol, respectively. Obviously, a much smaller mesh size or time step provides much more accurate results, but at the expense of much CPU time. The optimal solution is considered the one for which σ is less than 0.5%.

Table 2 Standard deviation σ(%) of various calculated dimensionless temperature histories with the optimal solution for mercury

ΔFo	ΔZ	ΔR	σ,%
1.8×10^{-3}	0.085	0.017	0.2
2.6×10^{-3}	0.085	0.017	0.3 (optimal)
2.6×10^{-3}	0.085	0.034	3.1
2.6×10^{-3}	0.085	0.0085	0.1
2.6×10^{-3}	0.17	0.017	06.3
2.6×10^{-3}	0.0425	0.017	0.1
5.2×10^{-3}	0.085	0.017	13.6

Table 3 Standard deviation σ(%) of various calculated dimensionless temperature histories with the optimal solution for glycerol

ΔFo	ΔZ	ΔR	σ,%
2.3×10^{-5}	0.17	0.034	0.1
4.6×10^{-5}	0.17	0.034	0.43 (optimal)
4.6×10^{-5}	0.17	0.068	4.1
4.6×10^{-5}	0.17	0.017	0.2
4.6×10^{-5}	0.34	0.034	9.8
4.6×10^{-5}	0.085	0.034	0.8
9.2×10^{-5}	0.17	0.034	8.7

Method of Estimation of Thermophysical Properties

When the sample thermal conductivity λ_s and thermal diffusivity α_s are unknown a priori, it is impossible to compute the temperature field without additional information. This can be the recorded temperature of the thermistor during the experiment if it is available. Therefore, if we assume that we already have a measured temperature–time history of a thermistor surrounded by a medium, the problem of estimation of the thermal conductivity and diffusivity from Eqs. (1–10) and the measured temperature information is referred to as the parameter estimation problem.[33] Therefore, λ_s and α_s can be determined by a search for those values that yield the best agreement between the time-dependent temperature of the thermistor from the numerical model and that recorded during the experiment. Information about α_s is available in the transient-state part of the temperature–time history of the thermistor surrounded by a sample. Thermal conductivity λ_s can be estimated from the steady-state part, or from the transient state, provided that α_s (or thermal capacity) is already known. Hence, it is important to fix the range in the temperature–time history where λ_s and α_s are estimated. In the present study, the steady-state part will not be used because the main purpose is to propose a method for simultaneous estimation of thermal conductivity and thermal diffusivity for liquids and moist porous materials. Use of the transient state will avoid natural convection effects for liquids and the migration of the moisture from the hot to cold regions in the presence of moist porous samples. These effects will lead to a serious error of estimation of λ_s and α_s.

Basic Equations

Based on the numerical results, the following procedure is proposed to determine simultaneously the thermal conductivity λ_s and the thermal diffusivity α_s of a porous sample or a liquid. As shown in Figs. (4–9), the dimensionless volume-averaged temperature of thermistor chip increases linearly from $Fo = 1$ to $Fo = 10$. Therefore,

in this time range, the effects of the thermistor's heat capacity and heat loss from lead wires are regarded as negligible. The numerical results in this time range are approximated by a linear equation, Eq. (12), and the coefficients A and B are determined by the least-squares method:

$$\theta_v = A + B \cdot \ell_n Fo \tag{12}$$

In the proceding time range, which, in dimensional form, depends on the nature of the sample, the measured temperature rise of a thermistor if it is available is also approximated by a linear equation with coefficients a and b as

$$T_v = a + b \cdot \ell_n t \tag{13}$$

where T_v is the volume-averaged temperature of the thermistor chip.

Estimation Procedure

To determine simultaneously the thermal conductivity and thermal diffusivity from one single measurement, two different forms of the measured temperature rise of thermistor are used. The first form is the plot of the measured temperature vs the logarithm of the dimensionless time Fourier number ($\ell_n Fo$). The second form is the plot of the same measured temperature vs the logarithm of time ($\ell_n t$). From the first plot, thermal diffusivity will be determined, whereas from the second, and by comparison with the numerical results, thermal conductivity will be determined. The plot of the measured temperature rise vs $\ell_n Fo$ will give an equation of the form

$$T_v = a' + b' \cdot \ell_n Fo \tag{14}$$

Observation of Eq. (14) shows that this equation is similar to Eq. (13) because the development of the logarithm of Fourier number will give

$$T_v = b' \cdot \ell_n t + \left(b' \ell_n \alpha_s \big/ r_{ch}^2 + a'\right) \tag{15}$$

Comparison between Eqs. (13) and (15) shows that the slopes are similar, $b = b'$, and that the intercepts are related through the relation

$$a = a' + b \ell_n \alpha_s \big/ r_{ch}^2 \tag{16}$$

Step 1. Evaluation of α_s

Because Eq. (13) is similar to Eq. (14), a plot of the measured temparature vs the logarithm of Fourier number will give a straight line if the Fourier number has the correct value. This means that it is possible to find the correct value of the Fourier number by the use of an iterative procedure by variation of the Fourier until the regression coefficient for the straight line fit of T_v vs $\ell_n Fo$ reaches its maximum. Once such a condition is satisfied, thermal diffusivity α_s can be calculated by the use of $\alpha_s = r_{ch}^2 Fo/t$ if r_{ch} the radius of the chip is already known.

Step 2. Evaluation of λ_s

Once α_s is determined, it will be used as known parameter in Eqs. (9) and (10). Thermal conductivity λ_s is evaluated by a parameter estimation procedure.[33] It is based on a comparison between the simulated and measured volume-averaged temperatures vs the logarithm of time $\ell_n t$. The difference or the error between them is evaluated by the deviation μ and the standard deviation σ in the least-square sense, which is given as

$$\mu = \left(\frac{1}{n}\right) \cdot \sum_{i=1}^{n} \mathrm{dev}_i, \qquad \sigma = \left(\frac{1}{n}\right) \cdot \sum_{i=1}^{n} \sqrt{(\mathrm{dev}_i)^2} \tag{17}$$

where $\mathrm{dev}_i = (T_{\exp i} - T_{\mathrm{cal}\, i})/T_{\exp i}$ and n is the number of time steps. $T_{\exp i}$ and $T_{\mathrm{cal}\, i}$ are the measured and calculated temperatures–time histories corresponding to time i.

After an initial guess of the thermal conductivity is given, the numerical volume-averaged temperature of the thermistor can be calculated and compared to the measured one. If the value of the standard deviation is less than the selected convergence criteria, the convergence is reached, otherwise, corrections for the input value of λ_s will be done, and the calculation will continue repeatedly until σ reaches the minimum value corresponding to the expected true thermal conductivity λ_s. The deviation μ is also used to correct the value of the thermal conductivity. If $\mu > 0$, this means that $T_{\exp} > T_{\mathrm{cal}}$; therefore, the value of thermal conductivity should be decreased to increase the mean temperature of the chip. If $\mu < 0$, the value of the thermal conductivity should be increased to reduce the deviation.

By the use of Eq. (9), a dimensional form for Eq. (12) can be written as

$$T_v = \left(q_v r_{ch}^2 \big/ \lambda_s\right) B \cdot \ell_n t + q_v r_{ch}^2 \big/ \lambda_s \cdot \left[B \cdot \ell_n \left(\alpha_s \big/ r_{ch}^2\right) + A\right] \tag{18}$$

By comparison of Eqs. (13) and (18), the thermal conductivity and thermal diffusivity can also be expressed as functions of coefficients *A, B, a, b,* the length of the chip L_{ch} and its radius r_{ch} (for the simulated cylindrical shape of the thermistor), and V and I, the voltage and current supplied to the chip, respectively, as

$$\lambda_s = q_v r_{ch}^2 (B/b) = (V I/\pi L_{ch}) \cdot (B/b) \tag{19}$$

$$\alpha_s = r_{ch}^2 \exp(a/b - A/B) \tag{20}$$

If the length of the chip L_{ch} and its radius r_{ch} are known from the calibration of the thermistor, the voltage V and the current I from the experiment, thermal conductivity, and diffusivity can be evaluated. Equations (19) and (20) are used to check the value of the thermal conductivity and diffusivity obtained by the use of the iterative process.

Conclusions

A device originally designed to measure the thermal conductivity of perfused biological tissue was evaluated for its applicability to the simultaneous estimation of thermal conductivity and thermal diffusivity of liquids and porous materials such as powders. In the present research, a numerical approach is used to calculate the temperature field of a thermistor surrounded by a medium of cylindrical shape. The thermal conductivity and diffusivity are estimated simultaneously by the use of an inverse method. It was also demonstrated that the amount of heat conducted through the lead wires increases with a decrease of the medium thermal conductivity. This seriously affects the accuracy of the estimated data of λ_s and α_s if it cannot be evaluated, as was the case in the conventional thermistor technique. Thermal conductivity and diffusivity are estimated with a time range selected in the transient-state part of the time-dependent temperature rise of the thermistor. In the dimensionless form, and for the presently used thermistor (Shibaura Electric. Company, Inc., PSB-S7), it is situated from $Fo = 1$ to $Fo = 10$. In dimensional form, and in the case of real measurements, this leads to a significant reduction of the applicable measurement time. Therefore, the interferences of thermal convection for liquids of low viscosity, or the migration of moisture within moist porous samples, are expected to be avoided. In addition, the differences between the real structure of thermistor and the present two-dimensional numerical model, as well as the time constant due to thermistor heat capacity, are minimized by exclusion of the time-range situated from $Fo = 0$ to $Fo = 1$. Finally, the numerical results reveal one of the main advantages of the present method: It always allows for a small sample, regardless the nature of the material, without affecting the accuracy of the estimated thermal conductivity and thermal diffusivity by the boundary conditions. This method would be particularly suitable for laboratory measurements of porous materials, especially rare materials such as those in planetary science.

References

[1] Presley, M. A., and Christensen, P. R., "Thermal Conductivity of Particulate Materials—A Review," *Journal of Geophysical Research*, Vol. 102, No. E3, 1997, pp. 6535–6549.

[2]Huang, L., and El-Genk, M. S., "Thermal Conductivity Measurements of Alumina Powders and Molded Min-K in Vacuum," *Journal of Energy Conversion and Management*, Vol. 42, No. 3, 2001, pp. 599–612.

[3]Griesinger, A., Spindler, K., and Hahne, E., "Measurements and Theoretical Modeling of the Effective Thermal Conductivity of Zeolites," *International Journal of Heat and Mass Transfer*, Vol. 42, No. 23, 1999, pp. 4363–4374.

[4]Ould Lahoucine, C., Sakashita, H., and Kumada, T., "Measurements of Thermal Conductivity of Buffer Materials and Evaluation of Available Correlations Predicting It," *Nuclear Engineering and Design*, Vol. 216, Nos. 1–3, 2002, pp. 1–11.

[5]Kumada, T., and Kobayasi, K., "Device and Method of Measuring Thermophysical Properties by Stepwise Heating," *Journal of Nuclear Science and Technology*, Vol. 12, No. 3, 1975, pp. 154–160.

[6]Sun, J., Longtin, J. P., and Irvine, T. F., Jr., "Laser-Based Thermal Pulse Measurement of Liquid Thermophysical Properties," *International Journal of Heat and Mass Transfer*, Vol. 44, No. 3, 2001, pp. 645–657.

[7]Nagai, H., Rossignol, F., Nakata, Y., Tsurue, T., Suzuki, M., and Okutani, T., "Thermal Conductivity Measurement of Liquid Materials by a Hot-Disk Method in Short-Duration Microgravity Environments," *Material Science and Engineering—A*, Vol. A276, Jan. 2000, pp. 117–123.

[8]Nagasaka, Y., and Nagashima, A., "Simultaneous Measurement of the Thermal Conductivity and the Thermal Diffusivity of Liquids by the Transient Hot-Wire Method," *Review of Scientific Instruments*, Vol. 52, No. 2, 1981, pp. 229–232.

[9]Griesinger, A., Spindler, K., and Hahne, E., "Periodic Hot-Wire Method for the Measurement of the Thermal Conductivity and Thermal Diffusivity of Small Quantities," *Heat and Mass Transfer*, Vol. 32, No. 6, 1997, pp. 419–425.

[10]Nakamura, S., Hibiya, T., and Yamamoto, F., "New Sensor for Measuring Thermal Conductivity in Liquid Metal by Transient Hot-Wire Method," *Review of Scientific Instruments*, Vol. 59, No. 6, 1988, pp. 997–999.

[11]Nakamura, S., Hibiya, T., and Yamamoto, F., "Ceramic Probe for Measuring the Thermal Conductivity of an Electrically Conductive Liquid by Transient Hot-Wire Method," *Review of Scientific Instruments*, Vol. 59, No. 12, 1988, pp. 2600–2603.

[12]Carslaw, H. S., and Jaeger, J. C., *Conduction of Heat in Solids*, 2nd ed., Oxford Univ. Press, Oxford, England, U.K., 1959, pp. 230–232.

[13]Blackwell, J. H., "The Axial-Flow Error in the Thermal Conductivity Probe," *Canadian Journal of Physics*, Vol. 34, No. 1, 1956, pp. 412–418.

[14]Xin-Gang, L., "The Boundary Induced Error on the Measurement of Thermal Conductivity by Transient Hot-Wire Method," *Measurement Science and Technology*, Vol. 6, No. 5, 1995, pp. 467–471.

[15]Jones, B. W., "Thermal Conductivity Probe: Development of Method and Application to a Coarse Granular Medium," *Journal of Physics E: Science Instruments*, Vol. 21, No. 9, 1988, pp. 832–839.

[16]Griesinger, A., Heidemann, W., and Hahne, E., "Investigation on Measurement Accuracy of the Periodic Hot-Wire Method By Means of Numerical Temperature Field Calculations," *International Communications in Heat and Mass Transfer*, Vol. 26, No. 4, 1999, pp. 451–465.

[17]Fujii, M., Zhang, X., Imaichi, N., Fujiwara, S., and Sakamoto, T., "Simultaneous Measurement of Thermal Conductivity and Thermal Diffusivity of Liquids Under Microgravity Conditions," *International Journal of Thermophysics*, Vol. 18, No. 2, 1997, pp. 327–339.

[18]Woodside, W., and Messmer, J. M., "Thermal Conductivity of Porous Media: I, Unconsolidated Sand," *Journal of Applied Physics*, Vol. 32, No. 9, 1961, pp. 1688–1691.

[19]Horai, K., Winkler, J. L., Jr., Keihm, S. J., Langseth, M. G., Fountain, J. A., and Weat, E. A., "Thermal Conductivity in a Composite Circular Cylinder: A New Technique for Thermal Conductivity Measurement of Lunar Core Samples," *Philosophical Transactions of the Royal Society of London, Series A: Mathematical and Physical Sciences*, Vol. A 293, No. 1406, 1980, pp. 571–598.

[20]Seiferlin, K., Banaskiewicz, T., Spohn, T., Kömle, N., and Kargl, G., "Line Heat-Source Measurements of the Thermal Conductivity of Porous H2O Ice, CO2 Ice and Mineral Powders Under Space Conditions," *Planetary and Space Science*, Vol. 44, No. 7, 1996, pp. 691–704.

[21]Nicolas, J., Andre, P., Rivez, J. F., and Debbault, V., "Thermal Conductivity Measurements in Soil Using an Instrument Based on the Cylindrical Probe Method," *Review of Scientific Instruments,* Vol. 64, No. 3, 1993, pp. 774–780.

[22]Hahne, E., and Kallweit, J., "Thermal Conductivity of Metal Hydride Materials for the Storage of Hydrogen: Experimental Investigation," *International Journal of Hydrogen Energy*, Vol. 23, No. 2, 1998, pp. 107–114.

[23]Wechsler, A. E., and Glaser, P. E., "Pressure Effects on Postulated Lunar Materials," *Icarus*, Vol. 4, No. 4, 1965, pp. 335–352.

[24]Fountain, J. A., and West, E. A., "Thermal Conductivity of Particulate Basalt as a Function of Density in Simulated Lunar and Martian Environments," *Journal of Geophysical Research*, Vol. 75, No. 20, 1970, pp. 4036–4069.

[25]Chato, J. C., "A Method for the Measurement of Thermal Properties of Biological Materials," *Thermal Problem in Biotechnology*, edited by J. C. Chato, American Society of Mechanical Engineers, New York, 1968, pp. 16–25.

[26]Balasubramaniam, T. A., and Bowman, H. F., "Thermal Conductivity and Thermal Diffusivity of Biomaterials: A Simultaneous Measurement Technique," *Journal of Biomechanical Engineering,* Vol. 99, No. K(3), 1977, pp. 148–154.

[27]Tervola, P., "A Method to Determine the Thermal Conductivity from Measured Temperature," *International Journal of Heat and Mass Transfer*, Vol. 32, No. 8, 1989, pp. 1425–1430.

[28]Lin, J. Y., and Cheng, T. F., "Numerical Estimation of Thermal Conductivity from Boundary Temperature Measurements," *Numerical Heat Transfer, Part A*, Vol. 32, No. 2, 1997, pp. 187–203.

[29]Ould Lahoucine, C., Sakashita, H., and Kumada, T., "Simultaneous Determination of Thermophysical Properties Using a New Thermistor Technique, Part 2: Experiment," *Journal of Thermophysics and Heat Transfer,* Vol. 18, No. 3, 2004, pp. 302–308.

[30]Patankar, S. V., "Numerical Heat Transfer and Fluid Flow," *Series in Computational Methods in Mechanics and Thermal Sciences*, Hemisphere, New York, 1980, pp. 52–54.

[31]Kurosaki, Y. (ed.), *JSME Data Book, Heat Transfer, Thermophysical Properties of Fluids*, 4th ed., Vol. 8, Japan Society of Mechanical Engineers, Tokyo, 1986, pp. 325–327.

[32]Lide, D. R., and Kehiaian, H. V., *CRC Handbook of Thermophysical and Thermochemical Data,* CRC Press, BocaRaton, FL, 1994, pp. 94, 417.

[33]Beck, J. V., and Blackwell, B., "Handbook of Numerical Heat Transfer," *Inverse Problems*, Wiley, New York, 1988, pp. 787–833.